Cytoplasmic Targeting Signals in Transmembrane Invariant Surface Glycoproteins of Trypanosomes*

Wei-Lien Chung‡, Mark Carrington§, and Mark C. Field‡¶

From the ‡Departments of Pathology and §Biochemistry, Tennis Court Road, University of Cambridge, Cambridge CB2 1QP, United Kingdom

Protein targeting mechanisms in flagellated protozoan parasites have received considerable interest because of a huge bias in these organisms toward the glycosylphosphatidylinositol anchor as a mechanism for the membrane attachment of cell surface macromolecules. In this study, the trafficking of invariant surface glycoprotein 65 (ISG65), a family of type I transmembrane proteins, was examined. Analysis of the C-terminal domains of ISG65 family members demonstrated a high level of conservation and, in particular, the presence of three lysine residues contained within the cytoplasmic tails of all ISG65s. ISG65 was expressed on the cell surface, in agreement with earlier work, but an intracellular pool of ISG65 was also detected within a Rab5A early endosome. Transplantation of the C-terminal 74 amino acids of ISG65 (encompassing the 23 C-terminal residues of the extracellular domain, the transmembrane peptide, and the cytoplasmic domain) onto the N-terminal domain of BiP (BiPN) was sufficient to target the chimera to the same internal compartments as native ISG65. Further, site-directed mutagenesis indicated that the cytoplasmic tail was required for endoplasmic reticulum exit and that at least two of the cytoplasmic domain lysine residues are needed for endosomal targeting, as removal of all three led to surface expression. Kinetic measurements demonstrate that the BiPN fusion protein (containing the ISG65 C terminus) has a short half-life, indicating rapid turnover. In contrast, BiPN fusion proteins containing a glycosylphosphatidylinositol anchor instead of the ISG65 C-terminal region are stably expressed on the surface, confirming the requirement for the ISG65 sequence for endosomal targeting. We suggest that the lack of surface expression of the BiPN-ISG65 fusion protein is likely due to more efficient internalization compared with ISG65. Taken together, these data demonstrate the presence of a lysine-dependent endocytosis signal in the ISG65 family.

The cell surface of the African trypanosome, *Trypanosoma brucei*, is dominated by glycosylphosphatidylinositol (GPI)[1]-anchored proteins (1) and is composed of a single GPI-anchored polypeptide species, the variant surface glycoprotein (VSG) (2). VSG occupies most of the surface membrane area forming a densely packed monolayer (3, 4). Numerous proteins are present on the trypanosome cell surface in addition to VSG, albeit at lower densities, and include membrane transporters, proteases, and receptors (5, 6, 7). Several families of cell surface proteins of unknown function, referred to as invariant surface glycoproteins (ISGs), are expressed exclusively in the bloodstream form (8, 9, 10). ISG100 is a polytopic protein partly resident within the endosomal system (11, 12), whereas the remainder of the characterized ISGs are type I transmembrane proteins with structural features similar to VSG (13). The trypanosome surface is rapidly turned over by a highly active endocytic system, which serves to internalize nutrients, including transferrin and low-density lipoprotein via specialized receptors. Significantly, VSG is also rapidly recycled (1, 14, 15), but the long half-life of VSG suggests that the protein is capable of multiple rounds of recycling (16).

The dominant mechanism of endocytosis in trypanosomes is mediated by clathrin, and this occurs exclusively from the flagellar pocket region (1, 17). VSG is not concentrated during incorporation into clathrin-coated pits, probably because of the high density on the cell surface precluding further concentration. Significantly, *T. brucei* lacks the genes for both the AP-2 complex and an endocytic dynamin (14, 18, 19, 20). Selectivity is present as distinct cargo molecules are located in early endosomes as defined by Rab5A and Rab5B (12). The mechanism for sorting is not known, but we have suggested that segregation may be based on the mode of membrane attachment (12). A putative signal for delivery of the flagellar pocket protein CRAM to the cell surface has been reported (20).

Here we have used the ISG65 family to initiate investigation of transmembrane domain surface protein trafficking in bloodstream-form trypanosomes. Sequences related to defined tyrosine-containing endocytic signals, *e.g.* NP*XX*Y and YKRF (21), are not present. Hence, if ISG65 does contain internalization motifs, these are likely to be distinct from those in metazoans and yeast. The ISG65 family has a highly conserved C-terminal region, particularly in the transmembrane and cytoplasmic regions, and includes three conserved lysines. Interestingly, conserved lysine residues are also found in the cytoplasmic domain of ISG75 (22) but not in the flagellar pocket-located transmembrane protein CRAM (20). To facilitate examination of the roles of the ISG65 C termini in protein

[1] The abbreviations used are: GPI, glycosylphosphatidylinositol; ISG, invariant surface glycoprotein; VSG, variant surface glycoprotein; TLCK, 1-chloro-3-tosylamido-7-amino-2-heptanone; HA, hemagglutinin; BiPN, N-terminal domain of BiP; ER, endoplasmic reticulum; TM, transmembrane; TES, 2-{[2-hydroxy-1,1-bis(hydroxymethyl)ethyl]amino}ethanesulfonic acid; DAPI, 4′,6-diamidino-2-phenylindole.

TABLE I

Sequences of synthetic oligonucleotides used in this study.

The following synthetic oligonucleotides were used for PCR. Sequences complementary to the target template are in upper case; additional sequences for cloning purposes are in lower case. Restriction sites are underlined, and mutagenic residues are in bold. All sequences are written 5′ to 3′.

Name	Sequence
FwGpi117	acgg<u>ctagc</u>AATGCTTGCAAAGATTCCTCT
RevGpi117	acgg<u>aattcc</u>taAAAAAGCAAGGCCGCAAA
FwGL117	acgg<u>ctagc</u>TGCAAGAAGGAGAGCAACTGC
FwTm	acgg<u>ctagc</u>GATGCTGACTTTGACTTTGACGGGTTG
RevTm	acgg<u>aattcc</u>taCATTACTACTTTTACGCT
FwTmD1	acgg<u>ctagc</u>GCAATGATTATATTGGCAGTC
RevTmD2	acgg<u>aattct</u>taCACCATTATGAAGAATGC
RevTmD4	acgg<u>aattcc</u>taCTGGGAGTTATTCCTCCT
RevTmD5	acgg<u>aattcc</u>taACCCTCCGCTTTTCCGGT
FwTmK1	acgg<u>ctagc</u>gATGCTGACTTTGACGGGTTGCTGGAGGCTGCCGAGGCTGCAGAGGTAACG**CGT**AGACATCAGCGTACGGCAATG
RevTmK2	acgg<u>aattcc</u>taCATTACTACTTTTACGCTAGAAACCCCACCCTCCGCTTTTCCGGTGTCCACATCCTGGGAGTTATTCCGTCG**ACG**CACCAT
RevTmK3	acgg<u>aattcc</u>taCATTACTACTTTTACGCTAGAAACCCCACCCTCCGC**ACG**TCCGGT
RevTmK4	acgg<u>aattcc</u>taCATTACTAC**GCG**CT
RevTmK234	acgg<u>aattcc</u>CTACATTACTAC**GCG**TACGCTAGAAACCCCACCCTCCGC**ACG**TCCGGTGTCCACATCCTGGGAGTTATTCCGTCG**ACG**CACCAT
FwBiPN	acgg<u>aattc</u>AACCCGGGAATTATG
RevBiPN	acgg<u>aattct</u>ta<u>gctagc</u>CGCGTAATCTGGGACGTC

targeting, we created a panel of fusion proteins containing the ISG65 C terminus attached to the N-terminal domain of BiP (23). Further, creation of a set of deletion and substitution mutants allowed dissection of trafficking signals within the ISG65 cytoplasmic domain. In addition, we revisited the hypothesis that the mode of membrane attachment functions to direct proteins to specific early endosomal compartments.

MATERIALS AND METHODS

Source and Culture of Bloodstream Forms of T. brucei—Bloodstream forms of MITat 1.2, derived from Lister strain 427 and expressing VSG 221, were cultured in HMI-9 medium (24), at 37 °C at 5% CO_2 in medical flats (Corning) in a humid atmosphere. Continued expression of VSG 221 was checked periodically by immunofluorescence and always approached 100%. The cells were quantitated with a Z2 Coulter Counter (Coulter Electronics) and maintained at densities between 10^5 and 5×10^6 cells/ml. Mutant trypanosomes were maintained in HMI-9 selection medium with 2.5 µg/ml G418 (Sigma) or phleomycin (Invitrogen), as was appropriate, for expression of ectopic ISG constructs.

Nucleic Acid and Recombinant DNA Methods—Standard molecular biology methods were carried out as described previously (25), unless otherwise indicated. Plasmids were grown in *Escherichia coli* XL1-Blue (Stratagene), unless otherwise described, following electroporation with a BTX600 ECM electroporator. PCR was performed using a 480 Thermal Cycler (PerkinElmer Life Sciences) with Herculase polymerase (Stratgene) and gel-embedded DNA purified using GeneClean (BIO101). The cloning vector pCR-Script was from Promega. The plasmids were prepared by using the Mini-prep spin kit (Qiagen). Oligonucleotide primers were obtained from Genosys and are detailed in Table I.

Construction of BiPN-ISG/VSG Fusion Protein Genes—All chimeric BiPN synthetic genes are shown schematically in Fig. 1. The bloodstream-form expression vector pXS5BiPN, containing a Geneticin cassette and an HA9-tagged N-terminal (ATPase) BiP cassette (BiPN-HA9), was a gift generously given by J. Bangs, University of Wisconsin (23). The C terminus of the BiPN-HA9 cassette was fused to either a GPI signal or transmembrane sequences using flanking NheI and EcoRI restriction sites. All these C-terminal signal sequences were generated by PCR from the genomic DNA of trypanosomes. The GPI signal sequence from VSG 117 (GPI(S)) was amplified using primers FwGpi117/RevGpi117. To ensure that processing of the GPI signal was not affected by being placed in an aberrant context, we also made a longer construct, GPI(L) with a 30-bp extension at the 5′-terminus, which was amplified using FwGL117/RevGpi117. The fragments were restricted by EcoRI and NheI and then ligated into pXS5BiPN to yield pXS5BiPNGPI(S) and pXS5BiPNGPI(L). Amplification of the C-terminal transmembrane (TM) sequence of ISG_{65} was performed with the primers FwTm/RevTm. The product was cloned into pXS5BiPN to generate pXS5BiPNTM. Sequencing confirmed that the construct corresponded to ISG65f and ISG65g isoforms (Fig. 1*A*). Deletions in the TM were made by reverse PCR of the whole pXS5BiPNTM. Three deletions in the cytoplasmic domain of TM were made with the forward primer FwBiPN and three reverse primers, RevTMD2, RevTMD4, and

RevTMD5, to generate pXS5BiPNTMΔ49–74, pXS5BiPNTMΔ58–74, and pXS5BiPNTMΔ66–74, respectively. pXS5BiPNTMΔ1–23 was generated with primers FwTmD1/RevBiPN to remove the ISG ectodomain region. pXS5BiPNTMΔ1–23Δ49–74 was made with primers FwTMD1/RevBiPN on the template pXS5BiPNTMΔ1–23. For introducing Lys to Arg mutations, five fragments with lysine substitutions were generated from pXS5BiPNTM by using the following primers: FwTMK1/RevTM for Lys-1, FwTM/RevTMK2 for Lys-2, FwTM/RevTMK3 for Lys-3, FwTM/RevTMK4 for Lys-4, and FwTM/RevTMK234 for Lys-234. Fragments were restricted and ligated into prepared pXS5BiPN vector. All constructs were verified by standard sequencing methods (MWG Biotech) prior to introduction into trypanosomes and were further verified by Western blotting.

Protein Electrophoresis and Western Blotting—Trypanosomes were harvested and washed twice in phosphate-buffered saline (Sigma). Pellets (10^7 cells) were lysed in 100 µl of boiling sample buffer and resolved by SDS-PAGE on 12% SDS-polyacrylamide minigels. The proteins were electrophoretically transferred onto nitrocellulose membranes (Amersham Biosciences) using a wet transfer tank (Hoefer Instruments). Equivalence of loading was verified by Ponceau Red (Sigma) staining of nitrocellulose membranes following transfer. Nonspecific binding was blocked with TBST (137 mM NaCl, 2.7 mM KCl, 25 mM Tris base, pH7.4, 0.2% Tween 20) supplemented with 5% freeze-dried milk. Antibodies were also diluted in TBST-milk. Rabbit polyclonal sera against anti-ISG65, anti-TbBiP (gift of J. Bangs, Madison, Wisconsin), and VSG 221 were diluted 1:10,000 in TBST-milk. A commercial monoclonal anti-HA9 (Santa Cruz Biotechnology) was used at 1:10,000. Incubations with commercial secondary anti-IgG rabbit or anti-IgG mouse horseradish peroxidase conjugates (Sigma) were performed at 10,000-fold dilution in TBST-milk. Bound antibodies were detected by chemiluminescence using the Amersham ECL detection system on Biomax MR-1 films (Kodak).

Immunofluorescence Analysis—Indirect immunofluorescence microscopy was performed as described previously (26). Antibodies were used at the following dilutions: rabbit and mouse anti-HA9 epitope IgG (both from Santa Cruz Biotechnology) at 1:1000, rabbit anti-ISG65 at 1:1000, rabbit anti-TbRAB5A (anti-5A, 12) at 1:100, rabbit anti-TbRAB11A (anti-11, 27) at 1:1000, mouse anti-p67 (anti-p67, J. Bangs, Madison) at 1:1000, rabbit anti-BiP at 1:1000 and rabbit anti-VSG 221 at 1:1000. The anti-ISG65 antisera do not recognize the chimeric BiPNTM constructs, as only the extracellular region, not including the sequences expressed here, was used to raise the antisera. This was confirmed by Western analysis (data not shown). Secondary antibodies, anti-rabbit Cy3 (Sigma) and anti-mouse Oregon Green (Molecular Probes), were used according the manufacturer's instructions. The cells were examined on a Nikon Eclipse E600 epifluorescence microscope fitted with optically matched filter blocks and a Photometrics CoolSnap FX CCD camera. Digital images were captured at 24-bit gray scale using Metamorph V3 (Universal Imaging Corp.) on a WindowsXP computer (Microsoft Inc.), and the resulting images were false-colored, merged, and assembled in Adobe PhotoshopCS (Adobe Systems Inc.).

Antibody Uptake—To stain for ISG65 and VSG 221 internalized into the cell, endocytosis of rabbit antiserum against either ISG65 or VSG 221 was allowed in living cells as follows. Bloodstream-form cells were
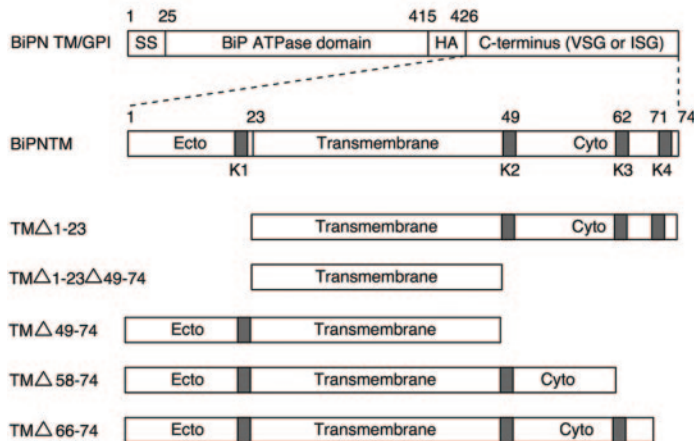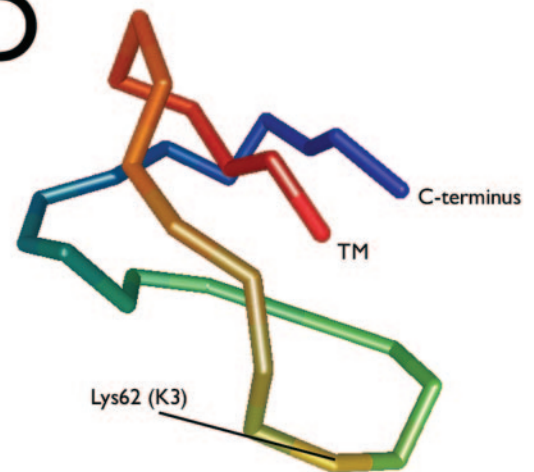
FIG. 1. **Conserved C-terminal sequences in ISG65 and design of membrane anchor BiPN constructs.** *A*, ClustalW alignment of ISG65 C-terminal regions, demonstrating absolute sequence conservation within the predicted transmembrane region (*underlined*) and high conservation in the cytoplasmic tail. The lysine residues are in *red* in ISG65–427. *Periods* indicate identity with ISG65–427. *B*, sequences of the parent constructs appended to the C terminus of BiPN. The HA epitope tag sequence used for identification is included. The lysine residues are in *red*, and the transmembrane domain is *underlined*. *Ecto* designates the C terminus of the ISG65 extracellular domain, *TM* is transmembrane, and *Cyto* is the cytoplasmic tail. Amino acid numbering, as used in the text, is indicated. For BiPNGPI, the spacer (*Spacer* or *Sp*) is indicated, and the GPI processing site is *underlined*. *C*, schematic of BiPNTM/GPI and deletion and substitution constructs. Numbering conventions are as in *B*, except for the *top schematic*, where absolute residue numbers (counting from the initiation Met) are given. Lysine residues are numbered Lys-1 (*K1*) to Lys-4 (*K4*) and also indicated by *gray blocks*. *Dotted lines* indicate expansion of the C-terminal region. *SS* is the N-terminal ER targeting signal sequence. *D*, predicted main chain structure of the cytoplasmic tail of ISG65–427, using three-dimensional PSSM. Three-dimensional PSSM suggests an open coiled structure, which indicates that most of the cytoplasmic tail is available for interaction with cytoplasmic trafficking factors. The C terminus and the position adjoining the transmembrane (*TM*) domain are indicated, and the main chain backbone is color-coded N to C terminus (*red* to *blue*).

harvested from 50-ml cultures at $1–2 \times 10^6$ cells/ml, pelleted at $800 \times g$ for 10 min, washed twice in 10 ml of phosphate-buffered saline, and resuspended in 1 ml of ice-cold serum-free HMI-9. The cells were incubated with 20 μl of anti-ISG65 or 10 μl of anti-VSG 221 at 4 °C for 30 min, and the cells were washed three times with ice-cold TES at 14,000 rpm for 20 s in a refrigerated microcentrifuge (Eppendorf) and

Targeting Signals in Surface Proteins of Trypanosomes

resuspended in HMI-9 and incubated for 0, 5, 10, and 20 min at 37 °C in 1.5-ml microtubes. The cells were again pelleted in the refrigerated microcentrifuge, and paraformaldehyde was immediately added to a final concentration of 3.5% for 30 min to fix the cells. The cells were then washed, spotted onto slides, permeabilized, blocked, and stained with Cy3-tagged anti-rabbit antibody as above.

GPI-phospholipase C (GPIPLC) Assay—1×10^7 cells were resuspended in 200 μl of ice-cold water containing 0.1 mM TLCK and held on ice for 5 min. After centrifugation at $3,000 \times g$ for 5 min, the supernatant was discarded. The cell ghosts were resuspended in 200 μl of 10 mM sodium phosphate buffer, pH 8.0, containing 0.1 mM TLCK. After incubation at 37 °C for 15 min, the sample was centrifuged at $16,000 \times g$ for 15 min, and the supernatant (*S*) and pellets (*P*) analyzed by Western blotting (see Fig. 3). This protocol quantitatively solubilizes cell surface GPI-anchored VSG during the 37 °C incubation by activating endogenous GPI-phospholipase C, which is GPI-specific under these conditions (28, 29). Most cytoplasmic proteins are released in the initial 0 °C lysis step.

Protein Stability—Trypanosomes were cultured for up to 4 h in HMI-9 medium containing 50 μg/ml cycloheximide (Sigma) to prevent translation. The samples were taken at different time points and analyzed by Western blot. Data were quantitated by scanning of x-ray films following chemiluminescence exposure on a Heidelberg 1200 scanner, followed by analysis with ImageJ (rsbweb.nih.gov/ij/download.html).

Bioinformatics—Sequences were aligned using ClustalW with default settings. Secondary and tertiary structure prediction and modeling was done using PSORT II (30) and three-dimensional position-specific scoring matrix (31) software. Predicted structures were loaded into iMOL (www.pirx.com/iMol) for further analysis and presentation.

RESULTS

The ISG65 Family Has a Conserved C-terminal Region—ClustalW alignment of the C-terminal regions of eight ISG65 family members indicated that, despite considerable variability within the ectodomains, the transmembrane and cytoplasmic regions are highly conserved (Fig. 1*A*). The predicted transmembrane regions are identical, and only a few conservative substitutions in the predicted cytoplasmic regions are found. Of additional interest was the presence of three fully conserved lysine residues in the cytoplasmic domain (*red* in Fig. 1*A*). Structural prediction using three-dimensional PSSM (31) suggested an open coiled structure for the cytoplasmic domain, with weak similarity to *Tityus serrulatus* toxin (Protein Data Bank, 1tsk) (32). Interestingly, this predicted structure has lysine 62 fully exposed and therefore could present most of its sequence to cytosolic proteins for interaction (Fig. 1*D*).

Design of ISG65 Reporter Constructs—ISG65 is most likely dimeric and encoded by a multigene family with a dimerization interface within the ectodomain.[2] This precludes the direct analysis of ISG65, as any mutant ISG65 isoform could form a heterodimer with endogenous ISG65. In addition, we have been unable to make ISG65 null mutants, and hence the experiments cannot be conducted in a null background.[2] Further, we wished to avoid any possibility of physiological interactions between the ISG65 ectodomain and other surface components. Therefore a set of chimeric reporter proteins were designed using the N-terminal domain of BiP (BiPN) (23), incorporating an HA epitope tag (Fig. 1*B*). BiPN is rapidly secreted from trypanosomes, indicating that the protein folds efficiently (33). BiPN has the further advantage of not normally being present on the trypanosome cell surface.

A full ISG65 transmembrane domain, including a short spacer region from the ectodomain to ensure preservation of correct membrane topology, was fused to BiPN (Fig. 1*C*, BiPNTM). A series of deletion constructs and substitution mutants, with one or more lysine residues changed to arginine, were also made (Fig. 1*C*). To compare the influence on intracellular transport of a GPI anchor *versus* a transmembrane domain, two GPI-anchored chimeric constructs containing the
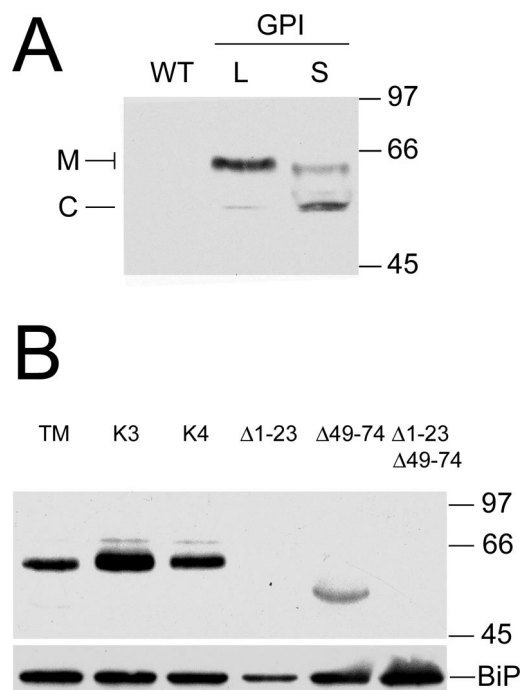

FIG. 2. **Expression of BiPN constructs in bloodstream-form trypanosomes.** *A*, GPI-anchored BiPN constructs. Western blot analysis of trypanosomes. *WT*, parental; *GPI L* and *S* indicate parasites transfected with BiPNGPI(L) and BiPNGPI(S), respectively. The membrane was probed with anti-HA9 antibodies. Note the absence of reactivity in the parental. *C* designates the predicted migration position of the GPI-anchored polypeptide without further modification and *M*, the maturate forms. *B*, transmembrane BiPN constructs. Western blot analysis of trypanosomes expressing BiPNTM and derivatives. The *upper panel* blot was probed with anti-HA9 antibodies. BiPN constructs are designated as in Fig. 1. Lys-3 and Lys-4 refer to Lys to Arg substitutions. Blots were reprobed with anti-TbBiP (*BiP*) as a loading control. Migration positions of molecular mass markers are indicated at right in kDa.
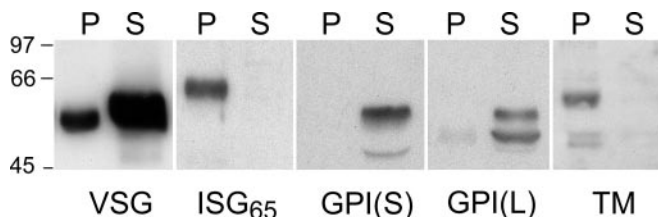

FIG. 3. **BiPNGPI constructs contain a GPI anchor.** Trypanosome lysates from untransfected parasites or cells expressing various BiPN constructs were subjected to a GPI-PLC release (see "Materials and Methods"), which converts GPI-anchored proteins to soluble forms (*S*). Uncleaved and transmembrane (*TM*) proteins are found in the pellet (*P*). VSG 221 and ISG65 were probed with the relevant antisera, and BiPN constructs were localized with anti-HA9. Migration positions of molecular mass markers are indicated at left in kDa.

VSG 117 GPI signal sequence were made and designated BiPNGPI(S) and BiPNGPI(L). BiPNGPI(L) includes an additional eleven residues of the VSG C-terminal domain to allay concern that efficient processing at the ω site (*underlined* in Fig. 1*B*) could be prevented by close proximity to the BiPN domain (Fig. 1*B*).

Expression of ISG65 Fusion Proteins in Trypanosomes—Following transfection and selection, lysates of transgenic parasites were analyzed by SDS-PAGE and Western blotting. Anti-HA monoclonals did not detect protein in wild-type trypanosomes but did react with lysates from cells transfected with both of the GPI-anchored BiPN chimeras (Fig. 2*A*). Interestingly, these proteins were expressed as more than one spe-

A HA   ISG   Merge

B HA   5A/11/p67   Merge

5A   A   B   C

11   D   E   F

p67   G   H   I
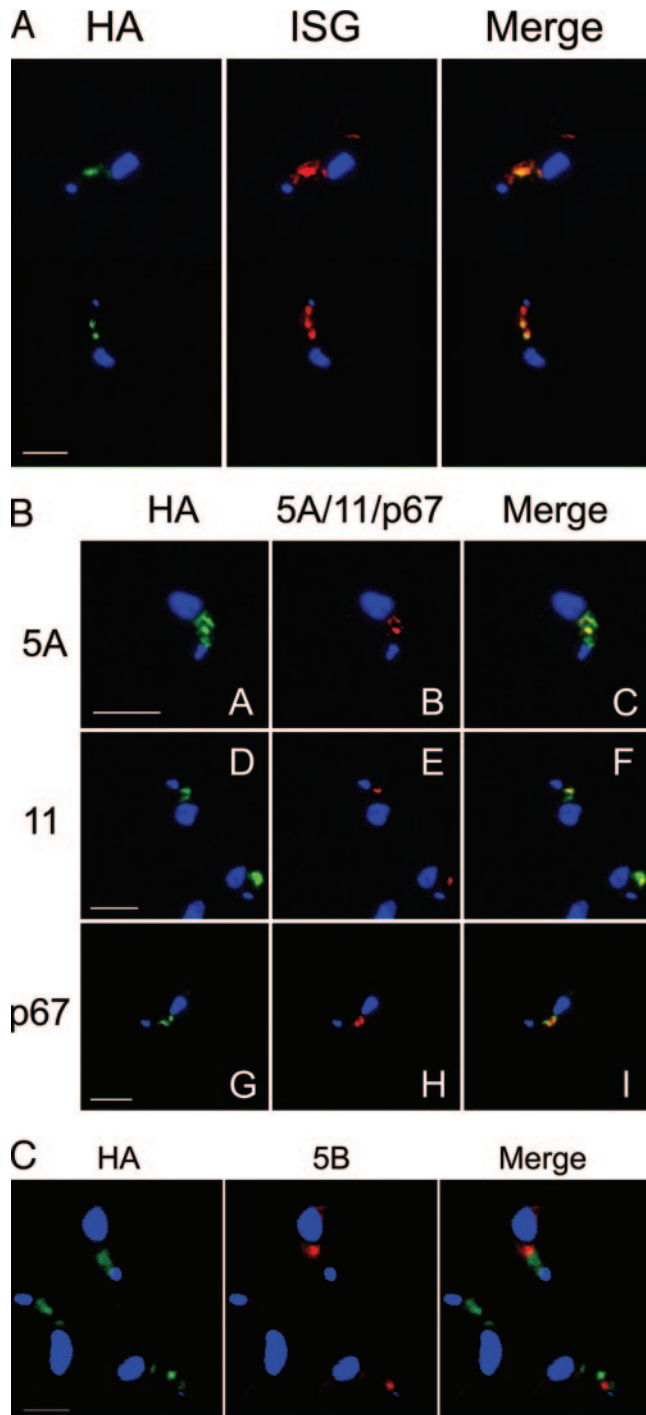
C HA   5B   Merge

FIG. 4. **BiPNTM and ISG65 are present within the endosomal recycling system.** *A*, immunofluorescence demonstrating colocalization of BiPNTM detected with anti-HA9 antisera (*green*) and ISG65 detected with anti-ISG65 antisera (*red*). DNA visualized with DAPI is in *blue*. *B*, BiPNTM colocalization with Rab5A, Rab11, and p67. In each set of panels, BiPNTM, detected with anti-HA9 antisera, is in *green* (*A*, *D*, and *G*) and Rab5A (*B*), Rab11 (*E*), and p67 (*H*) is in *red*. The merged images (*C*, *F*, and *I*) show clear colocalization for Rab5A and Rab11 (*yellow*). Note that for p67, the structures are juxtaposed but are distinct and superimposed in the Z plane but not colocalized. DNA visualized with DAPI is in *blue*. *Scale bar* is 5 μm. *C*, BiPNTM is not found in the Rab5B early endosome. Shown is immunofluorescence of BiPNTM detected with anti-HA9 antisera (*green*) and Rab5B detected with anti-Rab5B antisera (*red*). *Scale bar*, 2 μm.

cies; for BiPNGPI(L), the majority of immunoreactivity migrated at ~62 kDa rather than at ~50 kDa, as predicted from the polypeptide molecular mass. A low abundance species was
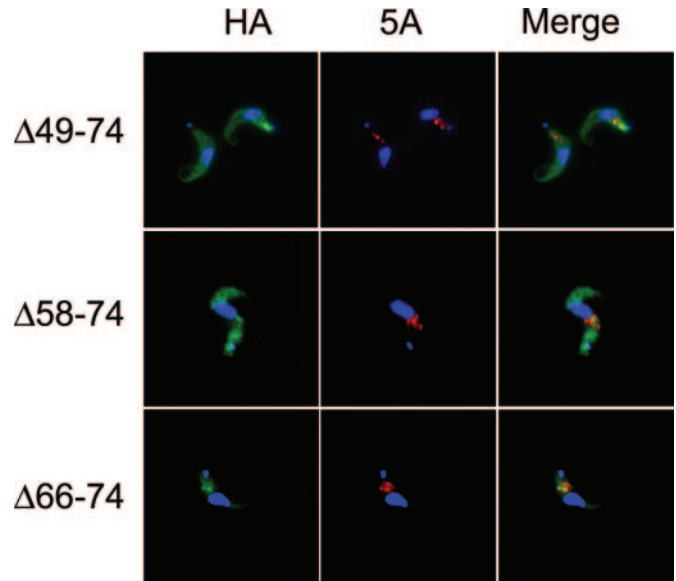

HA   5A   Merge

Δ49–74

Δ58–74

Δ66–74

FIG. 5. **Deletion of the cytoplasmic tail abrogates ER exit and endosomal targeting.** The location of the BiPNTM deletion constructs in permeabilized cells are shown in the *left panels*, visualized with anti-HA9 antibodies (*green*). Rab5A is shown in the *center panels* in *red*. The merge shows clear colocalization (*yellow*). DNA in the nucleus and kinetoplast, visualized with DAPI, is shown in *blue*. Only the Δ66–74 construct is significantly colocalized with Rab5A.

detected at this position on the blot, suggesting that the decreased migration was because of post-translational modification. Further, the BiPNGPI(S) chimera also presented as two bands, but in this case, the major form was the lower molecular mass species. As BiPN lacks an *N*-glycosylation site, the increased molecular mass is probably due to processing of the GPI anchor core glycan (34). Both isoforms in each case were efficiently solubilized by endogenous GPI-PLC (Fig. 3) and migrated with apparently lower molecular mass, consistent with removal of diacylglycerol. Hence BiPNGPI(L) and BiPNGPI(S) likely contain glycolipid anchors.

All of the lysine substitution mutants and most of the deletion mutants were also expressed in bloodstream-form trypanosomes (Figs. 2*B* and 5). These proteins migrated at the predicted molecular masses, and extensive post-translational modification is unlikely. The BiPNTM protein was also stably membrane-associated and fully resistant to solubilization by GPI-PLC (Fig. 3), consistent with the presence of a transmembrane anchor.

Of the deletion constructs, TMΔ1–23 and TMΔ1–23Δ49–74 were not detected, despite repeated transfections and generation of drug-resistant cells plus recovery of the construct from genomic DNA by PCR (data not shown). The results suggest that the C terminus of the ectodomain is required for stable expression to prevent ER-associated degradation (35, 36).

The ISG65 C Terminus Targets BiPN to the Endosome—BiPNTM was detected with HA antibody in permeabilized trypanosomes in structures in the posterior region of the cell, suggesting endosomal location (Fig. 4*A*). These structures also contained ISG65, indicating that the presence of the C terminus of ISG65 in BiPNTM was sufficient to target the protein to the same intracellular compartments as ISG65 itself. This was confirmed by co-staining with antibodies to Rab5A, Rab11, and p67 markers for early endosomes, recycling endosomes, and the lysosome, respectively (26, 27, 37). The HA stain co-localized with Rab5A and Rab11, indicating that the internal pool of BiPNTM was indeed within early and recycling endosomes (Fig. 4*B*). Cells co-stained with antibody to p67 showed close proximity of p67 and BiPNTM, but the compartments were
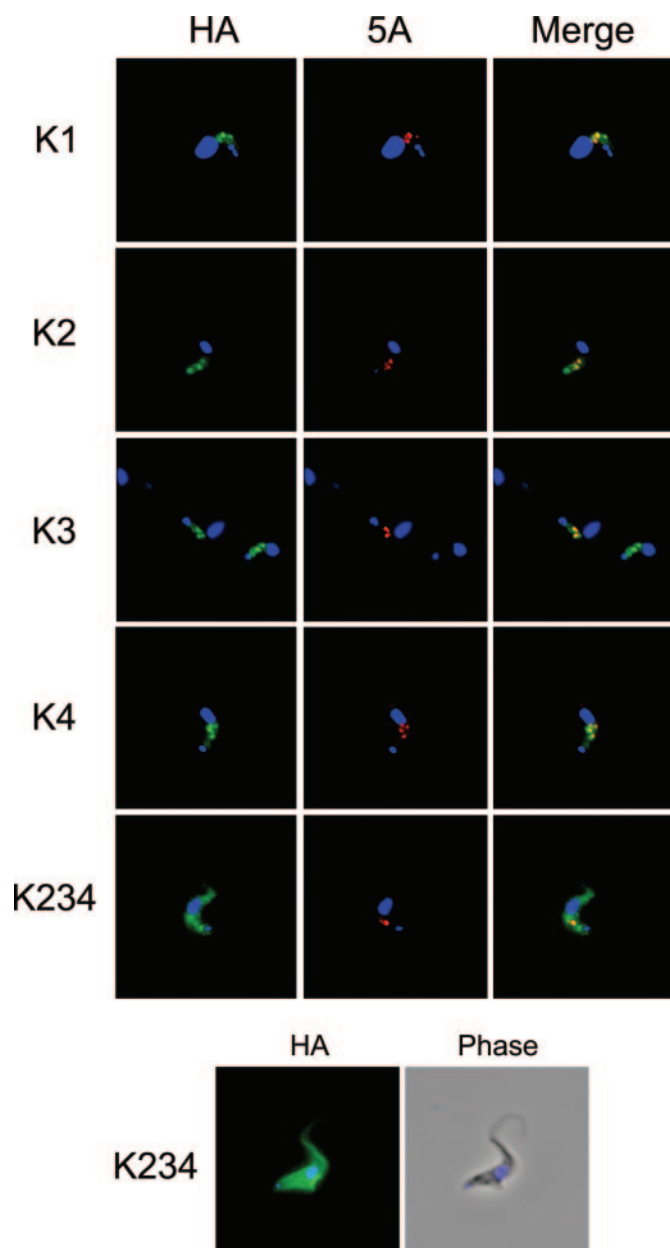
FIG. 6. **Lysines are required in the cytoplasmic tail of ISG65 to target to endosomes.** Localization, by immunofluorescence, of a panel of Lys to Arg substitution mutants of BiPNTM. Locations of the BiPNTM fusion proteins are shown at *left* in *green* (anti-HA9) and Rab5A in *red* at *center* in permeabilized cells. Deletion of all three lysine residues (K234) in the cytoplasmic tail results in mislocalization. *Bottom panel* shows immunofluorescence of nonpermeabilized trypanosomes expressing BiPNTMK234 on the surface.

distinct. Significantly, there was also no co-localization between BiPNTM and Rab5B (Fig. 4C). Taken together, these data show that BiPNTM is targeted to endosomal compartments and suggest that the C terminus of ISG65 is sufficient for faithful endosomal targeting. BiPNTM was not detected at the surface in nonpermeabilized cells.

Deletion Mutants Map a Region in the ISG65 Cytoplasmic Domain Required for Sorting—To examine in more detail the targeting information in the ISG65 C terminus, a set of deletion constructs was made (Fig. 1C). BiPNTMΔ49–74, which removed the entire cytoplasmic tail, was localized to a diffuse reticular network, consistent with failure to exit the ER (Fig. 5). Inclusion of an additional eight amino acids in BiPNTMΔ58–74 resulted in ER localization, but incorporation
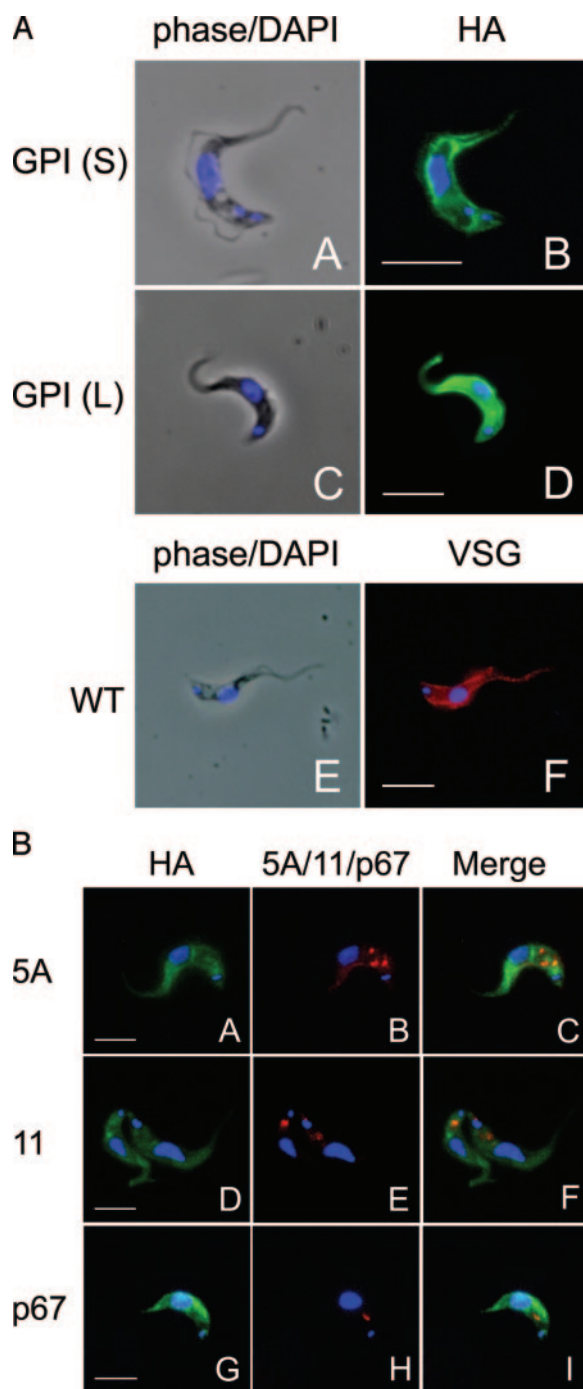

FIG. 7. **BiPNGPI is expressed in the surface and is not found in endosomal compartments.** *A*, immunofluorescence of nonpermeabilized cells demonstrating surface fluorescence for BiPN in the context of a GPI anchor. Constructs were visualized with anti-HA9 (*green*). For comparison, staining of 427 cells with anti-VSG 221 is shown (*E* and *F*). *B*, permeabilized cells expressing BiPNGPI(L) stained for HA9 (*green*, *A*, *D*, and *G*) and endosomal compartments (*red*, *B*, *E*, and *H*) with antibodies to Rab5A, Rab11, and p67 as indicated. *Scale bars*, 5 μm.

of a further eight residues (BiPNTMΔ66–74) led to targeting to the endosome. Hence the region between residues 58 and 65 is essential for ER exit. None of the C-terminal deletion constructs were detectable on the cell surface by immunofluorescence. Further, residues in the Δ66–74 mutant are sufficient for subsequent targeting to the endosome and amino acids 67–74, which include a single lysine (Lys-71), are dispensable.

Lysine Residues Are Required for Endosomal Delivery—In higher eukaryotes, modification of lysines by ubiquitin can
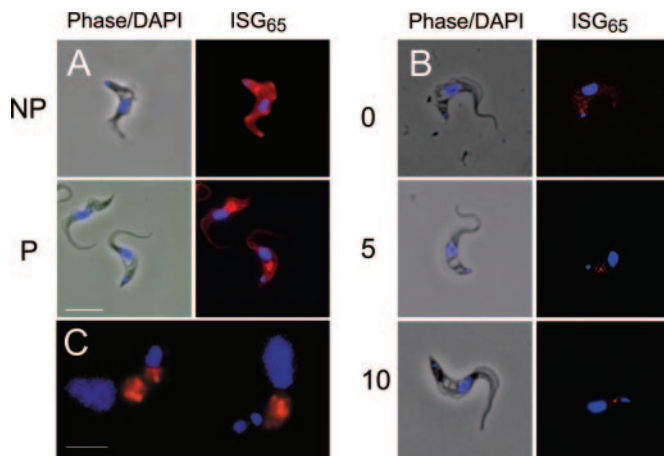
FIG. 8. **ISG65 can be capped and is present in endosomes.** *A*, ISG65 visualized in nonpermeabilized (*NP*) and permeabilized trypanosomes (*P*) with anti-ISG65 antibodies (*red*, *right panels*). *Scale bar* is 5 μm. *B*, internalization of anti-ISG65 antibodies by trypanosomes. Parasites were coated with antibody to ISG65 and allowed to internalize the antibody after washing. IgG was detected with anti-rabbit secondary antibody. Immunofluorescence is shown at *right* with IgG visualized in *red* at various times of internalization (in minutes). For comparison, internalized VSG antibody (*red fluorescence*) is shown in *C*. *Scale bar*, 2 μm.

FIG. 9. **BiPNTM has a short half-life.** Trypanosomes expressing BiPN or BiPNTM constructs were treated with cycloheximide and aliquots of cultures analyzed by Western blot with anti-HA or with anti-BiP. Both BiPN and BiPNTM are rapidly lost from the cell. Although BiPN is secreted (24), no BiPNTM was detected in culture supernatants, indicating that the protein was degraded intracellularly. The stability of BiP indicates that the cells remain intact and unstressed during these experiments. Time is indicated *above the lanes* in hours. Results are from single representative experiments, which have been performed at least twice. Quantitation of these and additional data are given in Table II.

TABLE II.
Stability of ISG65 and BiPN constructs

Trypanosomes were treated with cyclohexamide and whole cell lysates prepared at $t = 0$ and after 4 hours. The levels of BiPN constructs, endogenous BiP and ISG65 were determined by Western blot and densitometry. Data are expressed as percent remaining, with $t = 0$ as 100%. The experiment has been done twice with similar results.

Construct	Percent recovered at 4 hours
BiP	91.6
ISG65	34.9
BiPNTM	13.5
BiPN	8.3
BiPNTMK1	3.7
BiPNTMK2	6.8
BiPNTMK3	20.2
BiPNTMK234	42.7

form an endocytic signal (37). A panel of substitution mutants were generated where each or all three lysine residues were replaced with arginine (Fig. 1). Substitution of any one lysine did not lead to a detectable change in location, and the majority of HA stain remained co-localized with Rab5A, similar to the wild-type construct (Fig. 6). This is also consistent with faithful targeting of the BiPNTMΔ66–74 construct lacking Lys-71 (K4). By contrast, replacement of all three lysines in the cytoplasmic tail (K234) led to a distinct localization; BiPNTMK234 was found on the surface of nonpermeabilized cells. Therefore, BiPNTM is capable of surface expression, but a lysine-dependent signal from the ISG65 cytoplasmic domain can prevent plasma membrane localization. As deletion of any single lysine is tolerated, two lysine residues appear sufficient for correct targeting of BiPNTM to the endosome.

A GPI Anchor Does Not Target BiPN to the Endosome—To detect any influence of the ISG65 C-terminal region on BiPN localization beyond those analyzed above, GPI-anchored variants were also analyzed. In addition, these data allowed reevaluation of a differential endosome-targeting model based on the type of membrane attachment (12). Both BiPNGPI(S) and BiPNGPI(L) were expressed on the surface of nonpermeabilized parasites. BiPNGPI(L) in particular gave highly uniform staining over the cell surface (Fig. 7A). Hence BiPN can be efficiently incorporated into the plasma membrane as a GPI-anchored molecule. Further, analysis of BiPNGPI(L) in permeabilized cells demonstrated a distribution throughout the cytoplasm, most likely the ER. This did not include the endosomal system as judged by co-staining with antibodies to Rab5A, Rab11, and p67 (Fig. 7B). Hence BiPN itself lacks endosomal-targeting information and also demonstrates that there is no block to the export of BiPN to the cell surface.

Native ISG65 Has a Substantial Endosomal Pool—Co-localization of the BiPNTM construct with ISG65, Rab5, and Rab11 suggests the presence of an endosomal ISG65 population (Fig. 4). Analysis of permeabilized and nonpermeabilized trypanosomes confirmed the presence of both internal and surface pools; the internal pool was restricted to the endosomal posterior region (Fig. 8A). To test directly whether ISG65 could be endocytosed, cells were coated with anti-ISG65 antisera, extensively washed, and th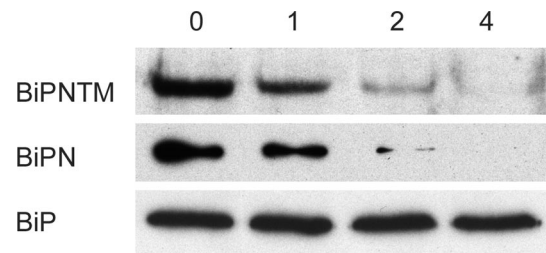en allowed to endocytose. The cells were fixed and the location of the antibody determined by immunofluorescence. At time zero, diffuse surface staining with some accumulation in the flagellar pocket was seen. At later times, staining became internal, and at 10 min, a clear endosomal localization was obtained (Fig. 8B), highly similar to internalized VSG antibody (Fig. 8C). The addition of nonspecific antibody did not result in accumulation of immunoglobulin within the endosomal system (data not shown).

Stability of ISG65 and BiPNTM Constructs—The presence of BiPNTM within the early endosome suggests that either the protein is actively recycled or is *en route* to later endosomal compartments. The stability of ISG65, BiPNTM, and several other proteins was directly assessed (Fig. 9, Table II). ISG65 itself has a short half-life, with >65% of the protein degraded within 4 h. BiPNTM was also short-lived. BiP, a long half-life ER protein, was essentially completely stable for the period of the experiment. As a further control, BiPN itself was monitored; this protein is efficiently secreted from trypanosome cells, consistent with previous studies (24). A single Arg to Lys substitution did not stabilize the protein, and in the case of the K1 and K2 mutants, may actually destabilize BiPNTM (Table II). By contrast, removal of all three lysine residues resulted in increased stability, consistent with a role for lysine in targeting to the endosomal system and also suggestive that BiPNTM is subject to an efficient degradation process that depends on endosomal targeting mediated by the ISG65 C terminus. The lower stability of BiPNTM compared with ISG65 is likely a consequence of its lack of surface expression. None of the BiPNTM constructs were detected in the medium, indicating that any turnover was due to intracellular degradation.

DISCUSSION

A substantial body of work has delineated the exocytic and endocytic pathway of VSG (1). Much less is known concerning endocytosis of transmembrane proteins, but the absence of an AP-2 complex and endocytic dynamin (19) suggests unusual mechanisms. Both the ISG65 and ISG75 proteins are expressed from multiple genes and are distributed over the whole cell surface (8, 9, 22, 37). Interestingly, although there is considerable sequence heterogeneity in the ectodomain, the C termini of both ISG65 and ISG75 protein families are highly conserved.

Endosomal Targeting Signals of ISG65—BiPNTM containing the entire C-terminal region of ISG65 fused to the N-terminal domain of BiP substantially colocalized with Rab5A and Rab11, indicating an endosomal location, further indicating that ISG65 is also present in Rab5A endosomes. Hence, the highly conserved cytoplasmic domain of ISG65 is a *bona fide* targeting signal, which is fully transplantable and sufficient for endosomal delivery of an irrelevant ectopic domain. This extends the cargo list for the trypanosome Rab5A early endosome to include internalized IgG, transferrin, VSG, and now ISG65 and therefore type I transmembrane proteins. Hence, discrimination of cargo cannot be based solely on GPI *versus* polypeptide anchoring mechanisms as proposed earlier (12). ISG100 remains the only molecule that has been localized to the Rab5B endosome; the function of the Rab5B endosome remains unclear but is essential.

ISG65 is able to endocytose and deliver bound antibody into the endosomal system in a manner similar to VSG (38). Previous studies suggested that ISG65 is inaccessible to antibody in live cells and that fixation is required for staining (37). The discrepancy between our data and the earlier work may be due to accumulation and concentration of antibody as used here, being more sensitive than simple surface staining. Also, recent work demonstrates a significant capacity for degradation of surface antibody (15, 38). The ability of ISG65 to be recognized by antibody on live cells has potential importance in evasion of the immune response, particularly in chronic infections, as the ISG family could represent a constant epitope recognized by host antibody. The capping and internalization of ISG antibody is therefore significant. Further work is required to evaluate this phenomenon *in vivo*.

BiPN anchored by GPI localized to the plasma membrane and was not found in the endosomal system, confirming that the ISG65 cytoplasmic domain is necessary for endosomal targeting. The presence of BiPNGPI on the surface indicates that BiPN has access to the plasma membrane. The high density of VSG on the plasma membrane may provide some degree of restriction in surface access, and the high prevalence of a VSG fold within additional surface molecules (including ISGs, ESAG6/7, and the serum resistance-associated protein) is consistent with this model (13, 39). However, the present study demonstrated that non-VSG molecules are accepted within the surface coat.

A Role for Lysine in ISG65 Trafficking—Deletion analysis indicates that the C-terminal nine residues are not required for exit from the ER and subsequent endosome delivery. This deletion removed the C-terminal lysine, independently demonstrated as dispensable in the K4 substitution mutant. Further, substitution of either K2 or K3 did not cause membrane mislocalization, but mutation of all three lysines in the K234 prevented endosomal targeting and resulted in surface expression. Together these data suggest that K2 and K3 are both required for correct function of the targeting signal. A role for lysine in endocytosis would be consistent with ubiquitination (37) and could explain the low stability of ISG65 and its rapid turnover. Protein ubiquitination has been described in

trypanosomes, and a large number of polypeptides are poly- and monoubiquitinated,[3] but a role in protein trafficking has not been reported.

ISG65 Is a Short-lived Protein—A short half-life suggests that ISG65 is unlikely to participate in multiple rounds of endocytosis/recycling. The basis for this rapid turnover appears to reside within the C terminus, as the BiPNTM chimera also has a short half-life. Although the function of ISG65 is unknown, the short half-life is inconsistent with a role as a nutrient receptor or as a structural protein. In higher eukaryotes, short half-life surface proteins, *e.g.* the epidermal growth factor receptor, are frequently components of signaling pathways, where degradation is essential for signal modulation (37), raising the possibility that ISG65 is also involved in signaling. Interestingly, ISG65 is slightly more stable than BiPNTM, consistent with an increased half-life due to a period of display on the cell surface. The failure of BiPNTM to be detectable on the surface could arise from either an intrinsic block in export of this class of protein or the efficient targeting of the construct to internal compartments. Two lines of evidence favor the last possibility; mutagenesis of all three lysines in the C-terminal tail or replacement of the transmembrane anchor with a GPI lipid results in efficient surface expression, suggesting that there is no intrinsic blockade to BiPN surface expression. ISG65 may be retained on the cell surface because of multiple low affinity and transient interactions with components of the surface coat or alternatively may interact with ectodomain-specific factors within the exocytic system. Clearly further work is required to investigate these possibilities.

REFERENCES

1. Grunfelder, C. G., Engstler, M., Weise, F., Schwarz, H., Stierhof, Y. D., Boshart, M., and Overath, P. (2002) *Traffic* **3,** 547–559
2. Ferguson, M. A., Homans, S. W., Dwek, R. A., and Rademacher, T. W. (1988) *Science* **239,** 753–759
3. Overath, P., Stierhof, Y., and Wiese, M. (1997) *Trends Cell Biol.* **1,** 27–33
4. Mehlert, A., Bond, C. S., and Ferguson, M. A. (2002) *Glycobiology* **12,** 607–612
5. El-Sayed, N. M., and Donelson, J. E. (1997) *J. Biol. Chem.* **272,** 26742–26748
6. Burchmore, R. J., Wallace, L. J., Candlish, D., Al-Salabi, M. I., Beal, P. R., Barrett, M. P., Baldwin, S. A., and de Koning, H. P. (2003) *J. Biol. Chem.* **278,** 23502–23507
7. Schell, D., Evers, R., Preis, D., Ziegelbauer, K., Kiefer, H., Lottspeich, F., Cornelissen, A. W., and Overath, P. A. (1991) *EMBO J.* **10,** 1061–1066; Correction (1993) *EMBO J.* **12,** 2990
8. Ziegelbauer, K., Multhaup, G., and Overath, P. (1992) *J. Biol. Chem.* **267,** 10797–10803
9. Ziegelbauer, K., and Overath, P. (1992) *J. Biol. Chem.* **267,** 10791–10796
10. Jackson, D. G., Windle, H. J., and Voorheis, H. P. (1993) *J. Biol. Chem.* **268,** 8085–8095
11. Nolan, D. P., Jackson, D. G., Windle, H. J., Pays, A., Geuskens, M., Michel, A., Voorheis, H. P., and Pays, E. (1997) *J. Biol. Chem.* **272,** 29212–29221
12. Pal, A., Hall, B. S., Nesbeth, D. N., Field, H. I., and Field, M. C. (2002) *J. Biol. Chem.* **277,** 9529–9539
13. Carrington, M., and Boothroyd, J. (1996) *Mol. Biochem. Parasitol.* **81,** 119–126
14. Grunfelder, C. G., Engstler, M., Weise, F., Schwarz, H., Stierhof, Y. D., Morgan, G. W., Field, M. C., and Overath, P. (2003) *Mol. Biol. Cell* **14,** 2029–2040
15. O'Beirne, C., Lowry, C. M., and Voorheis, H. P. (1998) *Mol. Biochem. Parasitol.* **91,** 165–169
16. Seyfang, A., Mecke, D., and Duszenko, M. (1990) *J. Protozool.* **37,** 546–552
17. Allen, C. L., Goulding, D., and Field, M. C. (2003) *EMBO J.* **22,** 4991–5002
18. Morgan, G. W., Hall, B. S., Denny, P. W., Carrington, M., and Field, M. C. (2002) *Trends Parasitol.* **18,** 491–496
19. Morgan, G. W., Hall, B. S., Denny, P. W., Field M. C., and Carrington, M. (2002) *Trends Parasitol.* **18,** 540–546
20. Morgan, G. W., Goulding, D., and Field, M. C. (2004) *J. Biol. Chem.* **279,** 10692–10701
21. Yang, H., Russell, D. G., Zheng, B., Eiki, M., and Lee, M. G. (2000) *Mol. Cell. Biol.* **20,** 5149–5163
22. Barak, L. S., Tiberi, M., Freedman, N. J., Kwatra, M. M., Lefkowitz, R. J., and Caron, M. G. (1994) *J. Biol. Chem.* **269,** 2790–2795

---

[3] P. Bastien and M. C. Field, unpublished data.

23. Ziegelbauer, K., Rudenko, G., Kieft, R., and Overath, P. (1995) *Mol. Biochem. Parasitol.* **69,** 53–63
24. Bangs, J. D., Brouch, E. M., Ransom, D. M., and Roggy, J. L. (1996) *J. Biol. Chem.* **271,** 18387–18393
25. Hirumi, H., and Hirumi, K. (1989) *J. Parasitol.* **75,** 985–989
26. Ausubel, F. M., Brent, R., Kingston, R. E., Moore, D., Seidman, J. G., Smith, J., and Struhl, K. (2003) *Current Protocols in Molecular Biology*, John Wiley and Sons, Inc.
27. Field, H., Farjah, M., Pal, A., Gull, K., and Field, M. C. (1998) *J. Biol. Chem.* **273,** 32102–32110
28. Jeffries, T. R., Morgan, G. W., and Field, M. C. (2001) *J. Cell Sci.* **114,** 2617–2626
29. Bangs, J. D., Andrews, N. W., Hart, G. W., and Englund, P. T. (1986) *J. Cell Biol.* **103,** 255–263
30. Butikofer, P., Ruepp, S., Boschung, M., and Roditi, I. (1997) *Biochem. J.* **326,** 415–423
31. Nakai, K., and Horton, P. (1999) *Trends Biochem. Sci.* **24,** 34–36
32. Kelley, L. A., MacCallum, R. M., and Sternberg, M. J. (2000) *J. Mol. Biol.* **299,** 499–520
33. Bangs, J. D., Ransom, D. M., McDowell, M. A., and Brouch, E. M. (1997) *EMBO J.* **16,** 4285–4294
34. Pinheiro, C. B., Marangoni, S., Toyama, M. H., and Polikarpov, I. (2003) *Acta Crystallogr. Sect. D Biol. Crystallogr.* **59,** 405–415
35. Zitzmann, N., Mehlert, A., Carrouee, S., Rudd, P. M., Ferguson, M. A., and Carroue, S. (2000) *Glycobiology* **10,** 243–249
36. Harley, C. A., Holt, J. A., Turner, R., and Tipper, D. J. (1998) *J. Biol. Chem.* **273,** 24963–24971
37. Field, M. C., Moran, P., Li, W., Keller, G. A., and Caras, I. W. (1994) *J. Biol. Chem.* **269,** 10830–10837
38. Kelley, R. J., Alexander, D. L., Cowan, C., Balber, A. E., and Bangs, J. D. (1999) *Mol. Biochem. Parasitol.* **98,** 17–28
39. Strous, G. J., and Gent, J. (2002) *FEBS Lett.* **529,** 102–109